Electronic Supplementary Information (ESI) for

Systematic centricity control using a chiral template: novel noncentrosymmetric polar niobium oxyfluorides and tantalum fluorides directed by chiral histidinium cations, [(L-hisH_2)$NbOF_5$], [(D-hisH_2)$NbOF_5$], [(L-hisH_2)TaF_7], and [(D-hisH_2)TaF_7]

HeeJung Choi and Kang Min Ok*

Department of Chemistry, Sogang University, 35 Baekbeom-ro, Mapo-gu, Seoul 04107, Korea

*E-mail: kmok@sogang.ac.kr

Table of contents

Section S1. Materials and Methods

Materials. ***Caution: HF solution is highly corrosive! Proper protective equipment is essential for safety.*** Nb_2O_5 (Junsei, 99.9%), Ta_2O_5 (Alfa Aesar, 99%), HF (Sigma Aldrich, 48 wt% aq. solution), L-histidine (Alfa Aesar, >98%), and D-histidine (Alfa Aesar, 99%) were purchased and used without further purification.

Syntheses of *L-Nb, D-Nb, L-Ta, and D-Ta*. Crystals of the reported compounds were grown by a slow evaporation method. First, clear Nb_2O_5/HF and Ta_2O_5/HF solutions were prepared. Two 0.133 g (0.5 mmol) portions of Nb_2O_5 and two 0.221 g (0.5 mmol) portions of Ta_2O_5 were placed in the respective 18 mL Teflon-cups containing 0.5 mL of HF (48 wt%) solutions. After putting the Teflon cups into stainless steel autoclaves and closing, the reactors were heated to 100 ℃ for 72 h. After cooling to room temperature, two 0.155 g (1 mmol) portions of L-histidine and two 0.155 g (1 mmol) portions of D-histidine were added to Nb_2O_5/HF and Ta_2O_5/HF solutions. Clear block-shaped crystals of [(L-hisH_2)$NbOF_5$] (***L-Nb***), [(D-hisH_2)$NbOF_5$] (***D-Nb***), [(L-hisH_2)TaF_7] (***L-Ta***), and [(D-hisH_2)TaF_7] (***D-Ta***) were grown in 7 days in in 94%, 97%, 91%, and 85% yields, respectively .

Figure S1. Experimental and calculated powder X-ray diffraction patterns of (a) ***L-Nb***, (b) ***D-Nb***, (c) ***L-Ta***, and (d) ***D-Ta***

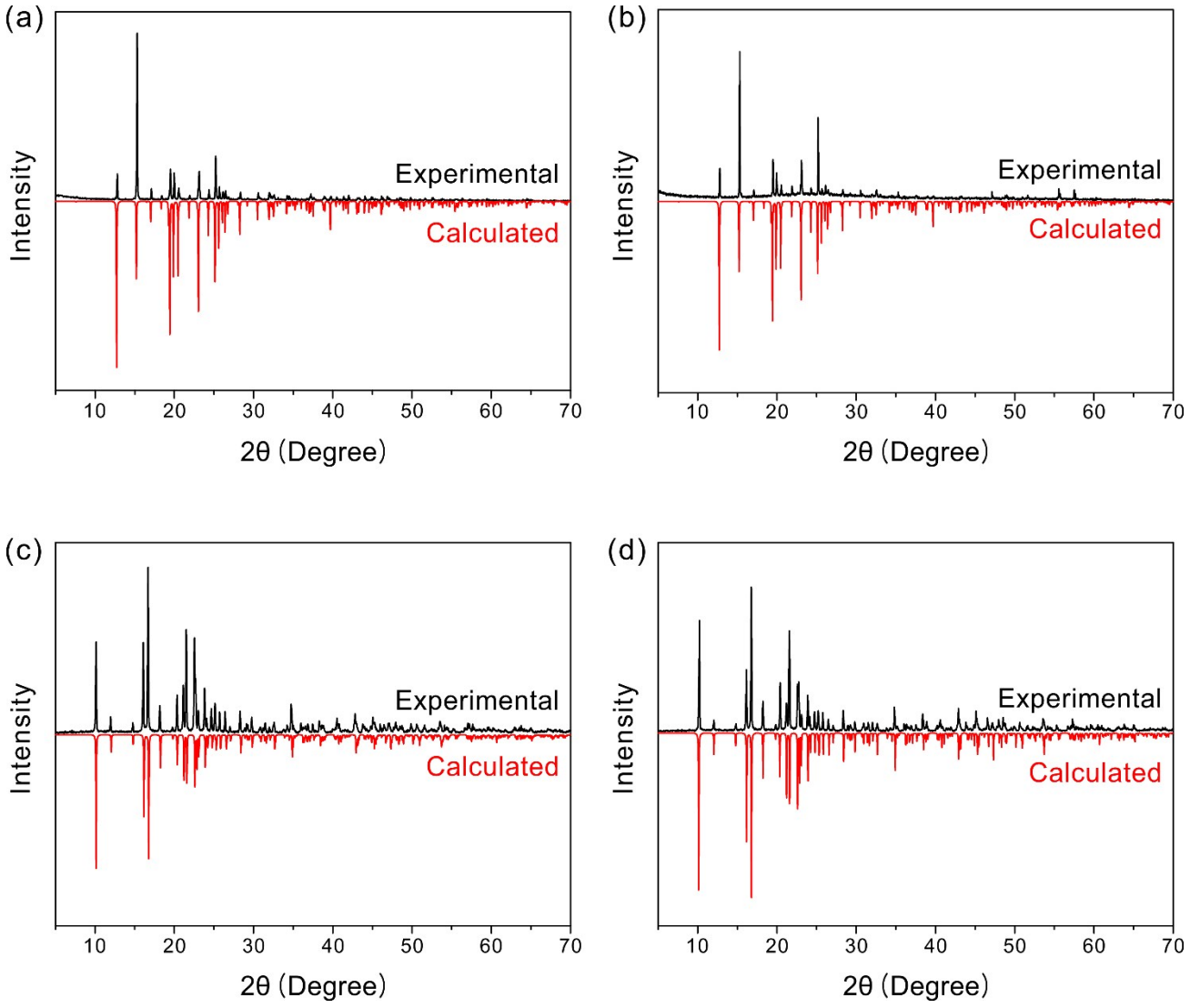

Instrumentation. Crystal structures of the reported compounds were determined by single crystal X-ray diffraction (SC-XRD). SC-XRD was conducted with a Bruker D8 QUEST diffractometer using graphite-monochromated Mo Kα (λ = 0.71073 Å) radiation and a PHOTON-II CPAD detector at 296 K at the Advanced Bio-Interface Core Research Facility, Sogang University. Colorless block-shaped crystals of ***L-Nb*** (0.168 mm × 0.252 mm × 0.316 mm), ***D-Nb*** (0.079 mm × 0.113 mm × 0.119 mm), ***L-Ta*** (0.105 mm × 0.195 mm × 0.389 mm), and ***D-Ta*** (0.065 mm × 0.078 mm × 0.171 mm) were selected to collect single crystal X-ray diffraction data. The collected data were integrated by the SAINT program.[1] Absorption correction was performed by the program SADABS.[2] The crystal structures were solved with SHELXS-2013[3] and refined with SHELXL-2013[4] implemented in WinGX-2014.[5]

Table S1. Crystallographic data for ***L-Nb, D-Nb, L-Ta,*** and ***D-Ta***

	L-Nb	***D-Nb***	***L-Ta***	***D-Ta***
fw	361.09	361.09	471.13	471.13
space group	$P2_1$	$P2_1$	$P2_1$	$P2_1$
a (Å)	5.4379(3)	5.4387(3)	7.8041(7)	7.8004(13)
b (Å)	8.6707(4)	8.6700(4)	8.2249(8)	8.2153(13)
c (Å)	11.7924(6)	11.7930(6)	9.2616(9)	9.2627(14)
α (°)	90	90	90	90
β (°)	99.2698(14)	99.276(2)	109.939(2)	109.890(4)
γ (°)	90	90	90	90
V (Å^3)	548.76(5)	548.81(5)	558.85(9)	558.17(15)
Z	2	2	2	2
T (K)	296	296	100	100
λ (Å)	0.71073	0.71073	0.71073	0.71073
ρ_{calcd} (g/cm^3)	2.185	2.185	2.800	2.803
$R(F_o)^a$	0.0157	0.0244	0.0129	0.0133
$R_w(F_o^2)^b$	0.0398	0.0449	0.0332	0.0312
Flack *x*	0.008(7)	0.046(15)	0.048(11)	-0.008(6)

$^a R(F) = \Sigma \, ||F_o| - |F_c|| \, / \, \Sigma \, |F_o|$.

$^b R_w(F_o^2) = [\Sigma w(F_o^2 - F_c^2)^2 \, / \, \Sigma w(F_o^2)^2]^{1/2}$.

Table S2. Selected bond distances (Å) for ***L-Nb***

Nb(1)-O(3)	1.787(2)	C(2)-O(2)	1.205(3)	C(6)-N(2)	1.316(4)
Nb(1)-F(1)	1.8973(16)	C(2)-O(1)	1.324(4)	C(6)-H(6)	0.9300
Nb(1)-F(2)	1.911(2)	C(3)-C(4)	1.503(4)	N(1)-H(1A)	0.8900
Nb(1)-F(3)	1.9447(19)	C(3)-H(3A)	0.9700	N(1)-H(1B)	0.8900
Nb(1)-F(4)	1.9613(19)	C(3)-H(3B)	0.9700	N(1)-H(1C)	0.8900
Nb(1)-F(5)	2.0687(19)	C(4)-C(5)	1.343(4)	N(2)-H(2N)	0.8600
C(1)-N(1)	1.488(4)	C(4)-N(2)	1.373(4)	N(3)-H(3N)	0.8600
C(1)-C(2)	1.516(4)	C(5)-N(3)	1.374(5)	O(1)-H(1O)	0.8200
C(1)-C(3)	1.540(3)	C(5)-H(5)	0.9300		
C(1)-H(1)	0.9800	C(6)-N(3)	1.314(6)		

Table S3. Hydrogen bonds distances (Å) for ***L-Nb***

D-H...A	d(D...A)	D-H...A	d(D...A)
N(1)-H(1A)...O(3)#1	2.854(4)	N(2)-H(2N)...F(5)#2	2.718(4)
N(1)-H(1B)...F(3)#2	2.756(3)	N(3)-H(3N)...F(5)#4	2.687(3)
N(1)-H(1C)...F(4)#3	2.755(3)	O(1)-H(1O)...O(3)	2.599(4)

Symmetry transformations used to generate equivalent atoms:
#1 -x+1,y-1/2,-z+2 #2 x+1,y-1,z #3 x,y-1,z #4 -x,y-1/2,-z+1

Table S4. Selected bond distances (Å) for ***D-Nb***

Nb(1)-O(3)	1.787(3)	C(2)-O(2)	1.203(5)	C(6)-N(2)	1.321(6)
Nb(1)-F(1)	1.893(2)	C(2)-O(1)	1.332(5)	C(6)-H(6)	0.9300
Nb(1)-F(2)	1.909(3)	C(3)-C(4)	1.500(5)	N(1)-H(1A)	0.8900
Nb(1)-F(3)	1.942(3)	C(3)-H(3A)	0.9700	N(1)-H(1B)	0.8900
Nb(1)-F(4)	1.958(3)	C(3)-H(3B)	0.9700	N(1)-H(1C)	0.8900
Nb(1)-F(5)	2.065(3)	C(4)-C(5)	1.339(6)	N(2)-H(2N)	0.8600
C(1)-N(1)	1.489(5)	C(4)-N(2)	1.377(6)	N(3)-H(3N)	0.8600
C(1)-C(2)	1.510(5)	C(5)-N(3)	1.374(6)	O(1)-H(1O)	0.8200
C(1)-C(3)	1.539(5)	C(5)-H(5)	0.9300		
C(1)-H(1)	0.9800	C(6)-N(3)	1.311(8)		

Table S5. Hydrogen bonds distances (Å) for ***D-Nb***

D-H...A	d(D...A)	D-H...A	d(D...A)
N(1)-H(1A)...O(3)#1	2.857(5)	N(2)-H(2N)...F(5)#3	2.721(5)
N(1)-H(1B)...F(4)#2	2.754(5)	N(3)-H(3N)...F(5)#4	2.689(5)
N(1)-H(1C)...F(3)#3	2.760(5)	O(1)-H(1O)...O(3)	2.601(5)

Symmetry transformations used to generate equivalent atoms:
#1 -x+1,y+1/2,-z #2 x,y+1,z #3 x-1,y+1,z #4 -x+2,y+1/2,-z+1

Table S6. Selected bond distances (Å) for ***L-Ta***

Ta(1)-F(2)	1.907(3)	C(1)-H(1)	1.0000	C(6)-N(3)	1.325(6)
Ta(1)-F(4)	1.937(3)	C(2)-O(2)	1.208(6)	C(6)-N(2)	1.333(6)
Ta(1)-F(3)	1.944(5)	C(2)-O(1)	1.318(6)	C(6)-H(6)	0.9500
Ta(1)-F(7)	1.955(4)	C(3)-C(4)	1.480(6)	N(1)-H(1A)	0.9100
Ta(1)-F(6)	1.971(3)	C(3)-H(3A)	0.9900	N(1)-H(1B)	0.9100
Ta(1)-F(5)	1.974(5)	C(3)-H(3B)	0.9900	N(1)-H(1C)	0.9100
Ta(1)-F(1)	1.985(4)	C(4)-C(5)	1.356(7)	N(2)-H(2N)	0.8800
C(1)-N(1)	1.494(5)	C(4)-N(2)	1.383(6)	N(3)-H(3N)	0.8800
C(1)-C(2)	1.518(6)	C(5)-N(3)	1.369(6)	O(1)-H(1O)	0.8400
C(1)-C(3)	1.556(7)	C(5)-H(5)	0.9500		

Table S7. Hydrogen bonds distances (Å) for ***L-Ta***

D-H...A	d(D...A)	D-H...A	d(D...A)
N(1)-H(1A)...F(1)#4	2.945(9)	N(1)-H(1C)...F(4)#1	2.881(4)
N(1)-H(1A)...F(5)#4	2.853(9)	N(2)-H(2N)...F(6)#1	2.761(5)
N(1)-H(1B)...F(6)#5	3.099(4)	N(3)-H(3N)...F(4)#2	2.969(5)
N(1)-H(1B)...O(2)	2.698(5)	N(3)-H(3N)...F(5)#3	2.824(6)
N(1)-H(1C)...F(3)#6	2.795(8)	O(1)-H(1O)...F(1)	2.573(5)

Symmetry transformations used to generate equivalent atoms:
#1 x+1,y,z+1 #2 x+1,y,z #3 -x+1,y-1/2,-z #4 -x+1,y-1/2,-z+1 #5 x,y,z+1 #6 -x+1,y+1/2,-z+1

Table S8. Selected bond distances (Å) for ***D-Ta***

Ta(1)-F(2)	1.913(3)	C(1)-H(1)	1.0000	C(6)-N(3)	1.329(6)
Ta(1)-F(4)	1.944(2)	C(2)-O(2)	1.218(5)	C(6)-N(2)	1.332(6)
Ta(1)-F(3)	1.952(4)	C(2)-O(1)	1.309(5)	C(6)-H(6)	0.9500
Ta(1)-F(7)	1.958(3)	C(3)-C(4)	1.481(6)	N(1)-H(1A)	0.9100
Ta(1)-F(5)	1.968(5)	C(3)-H(3A)	0.9900	N(1)-H(1B)	0.9100
Ta(1)-F(6)	1.974(2)	C(3)-H(3B)	0.9900	N(1)-H(1C)	0.9100
Ta(1)-F(1)	1.983(3)	C(4)-C(5)	1.362(6)	N(2)-H(2N)	0.8800
C(1)-N(1)	1.487(5)	C(4)-N(2)	1.381(6)	N(3)-H(3N)	0.8800
C(1)-C(2)	1.519(6)	C(5)-N(3)	1.373(6)	O(1)-H(1O)	0.8400
C(1)-C(3)	1.558(6)	C(5)-H(5)	0.9500		

Table S9. Hydrogen bonds distances (Å) for ***D-Ta***

D-H...A	d(D...A)	D-H...A	d(D...A)
N(1)-H(1A)...F(1)#1	2.951(8)	N(1)-H(1C)...F(6)#4	3.084(4)
N(1)-H(1A)...F(5)#1	2.857(8)	N(2)-H(2N)...F(6)#3	2.763(5)
N(1)-H(1B)...F(3)#2	2.781(7)	N(3)-H(3N)...F(4)#5	2.950(5)
N(1)-H(1B)...F(4)#3	2.889(4)	N(3)-H(3N)...F(5)#6	2.830(6)
N(1)-H(1C)...O(2)	2.703(4)	O(1)-H(1O)...F(1)	2.574(5)

Symmetry transformations used to generate equivalent atoms:
#1 -x+1,y+1/2,-z+1 #2 -x+1,y-1/2,-z+1 #3 x-1,y,z-1 #4 x,y,z-1 #5 x-1,y,z #6 -x+1,y+1/2,-z+2

Energy dispersive analysis by X-ray (EDX). EDX was performed using a Horiba Energy EX-250 instrument equipped on a Hitachi S-3400N scanning electron microscope. Crystals of the reported compounds were attached on a carbon tape and coated using Pt before mounting. The EDX data were consistent with the calculated atomic ratio from the single crystal X-ray diffraction (Figure S5).

Figure S2. SEM-EDX data for ***L-Nb, D-Nb, L-Ta,*** and ***D-Ta***

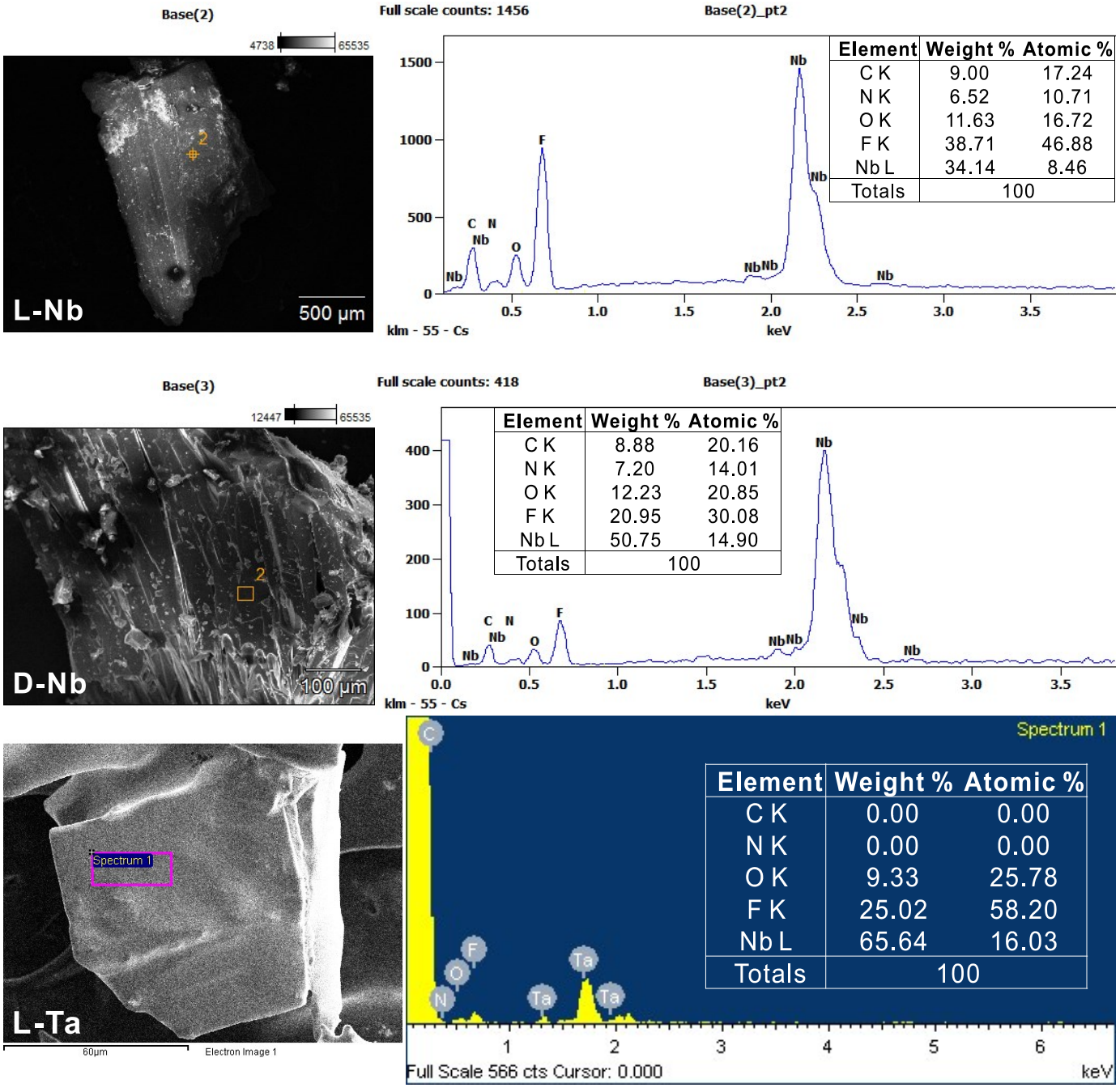

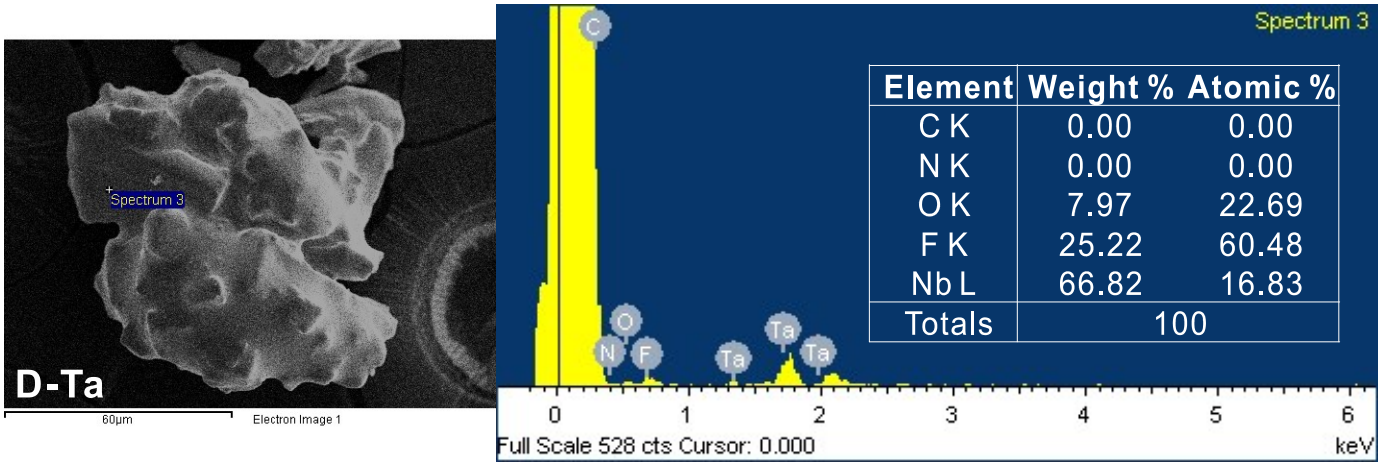

Element	Weight %	Atomic %
C K	0.00	0.00
N K	0.00	0.00
O K	7.97	22.69
F K	25.22	60.48
Nb L	66.82	16.83
Totals	100	

Elemental Analysis (EA). EA was carried out by a Thermo Finnigan Flash EA1112 on Sn capsule.

Table S10. EA data for ***L-Nb, D-Nb, L-Ta,*** and ***D-Ta***

Element	***L-Nb***	***D-Nb***	***L-Ta***	***D-Ta***
N	11.5424	11.5962	8.8754	8.8918
C	19.8598	19.9143	15.4809	15.2922
H	3.2766	3.0023	2.4891	2.1186
Totals	34.6789	34.5128	26.8454	26.3027

Infrared (IR) spectroscopy. FT-IR spectra were measured using a Thermo Scientific Nicolet iS50 FT-IR spectrometer with an attenuated total reflection (ATR) accessory in the range of 400–4000 cm^{-1}.

Figure S3. IR spectra for ***L-Nb , D-Nb, L-Ta,*** and ***D-Ta***

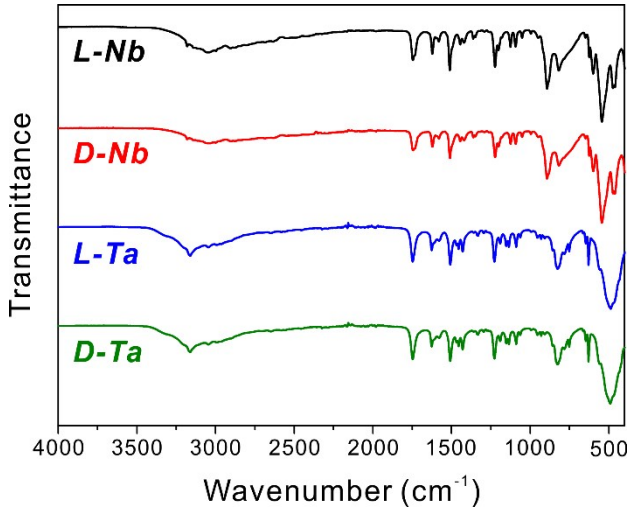

Ultraviolet-visible (UV-vis) diffuse-reflectance spectroscopy. UV-vis diffuse-reflectance spectra were obtained in the range of 200–900 nm by using a Lambda 1050 spectrophotometer. The band gap energy was calculated by the Kubelka-Munk function.

Figure S4. UV-vis diffuse reflectance spectra for ***L-Nb, D-Nb, L-Ta,*** and ***D-Ta***

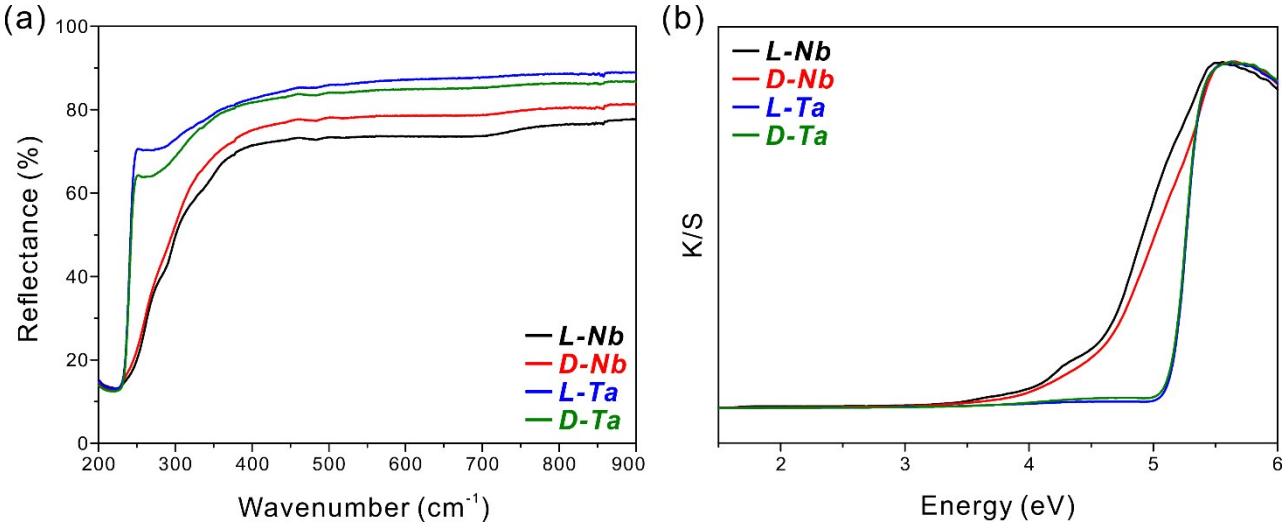

Thermogravimetric analyses (TGA). TGA was conducted by using a SCINCO TGA-N 1000 thermal analyzer. The ground samples were loaded in alumina crucibles and heated from room temperature to 900 °C at a rate of 10 °C min^{-1} under flowing air.

Figure S5. TGA diagrams for ***L-Nb, D-Nb, L-Ta,*** and ***D-Ta***

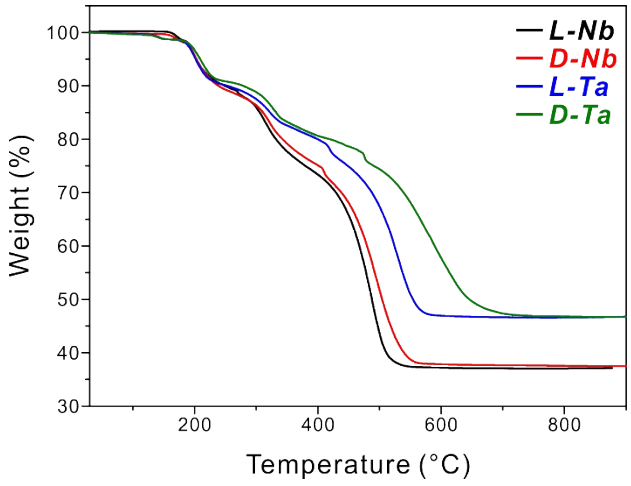

Density functional theory (DFT) calculations. DFT calculations were conducted to investigate the electronic structure in the Quantum Espresso package.[6] The crystal structure models obtained through SC-XRD measurement were utilized for structural optimization. The electronic structures of the compounds were calculated using the ultrasoft pseudopotentials[7] with nonlinear core correction. Also, the Perdew–Burke–Ernzerhof (PBE)[8] functional and the scalar relativistic effect were applied for all constituent elements (C, H, N, O, Nb, and Ta) from the Quantum Espresso website. For ***Nb*** compounds, the wave function and the charge energy of the cutoff energies for the self-consistent function (SCF) calculations were set to 49.146 and 326.261 Ry, respectively. While, the kinetic energy and charge density cutoff were set to 51.330 and 530.066 Ry, respectively for ***Ta*** compounds. The SCF convergence criterion was set to under 10^{-6} Ry and all DFT calculations were computed in 6 × 4 × 3 for ***Nb*** compounds and 4 × 4 × 3 for ***Ta*** compounds k-point grids of Brillouin zone.

Figure S6. Band structures for (a) ***L-Nb***, (b) ***D-Nb***, (c) ***L-Ta***, and (d) ***D-Ta***. Arrows represent the optical transition from the valence band maximum to the conduction band minimum.

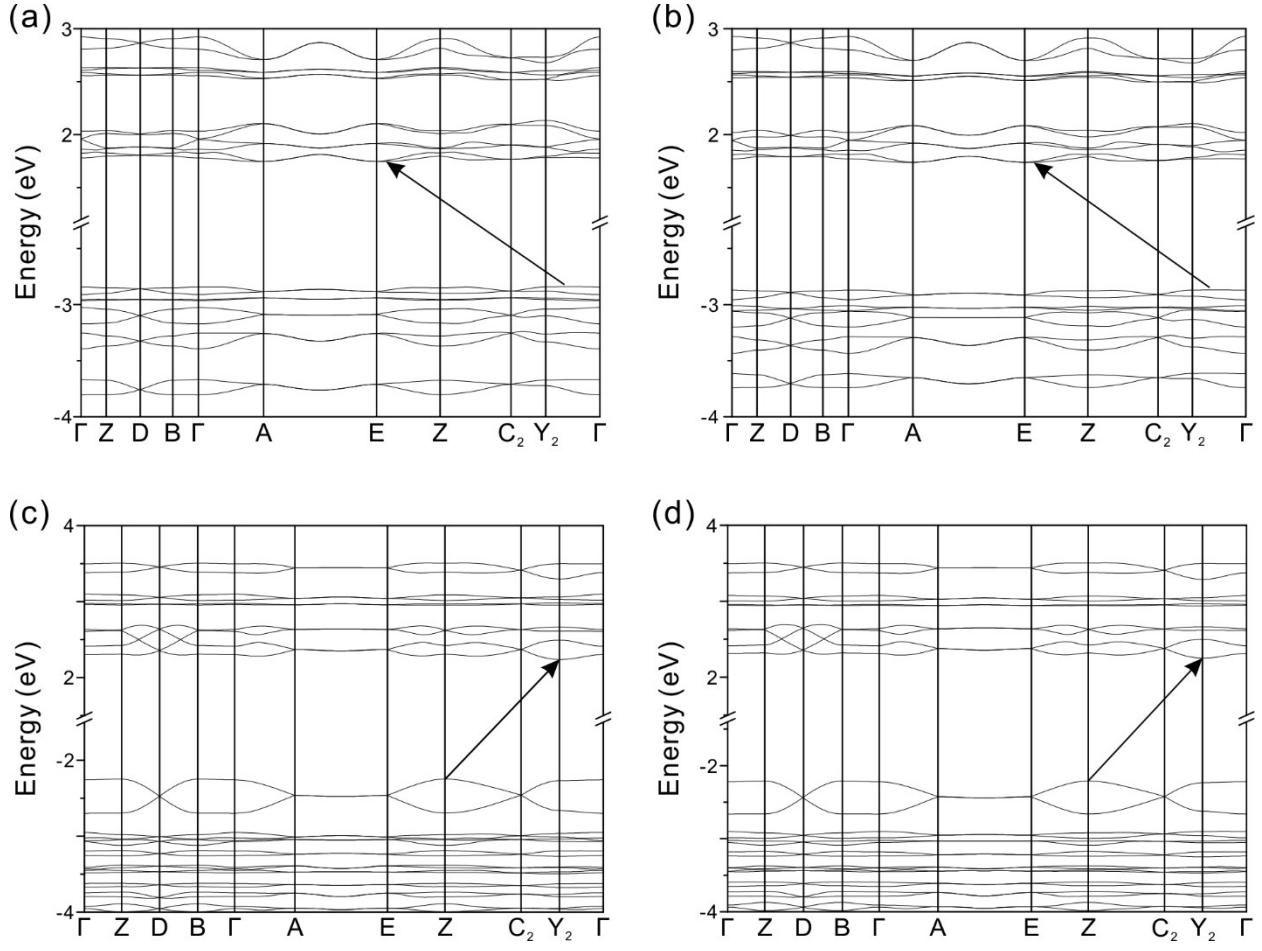

Figure S7. Density of states for (a) ***L-Nb***, (b) ***D-Nb***, (c) ***L-Ta***, and (d) ***D-Ta***.

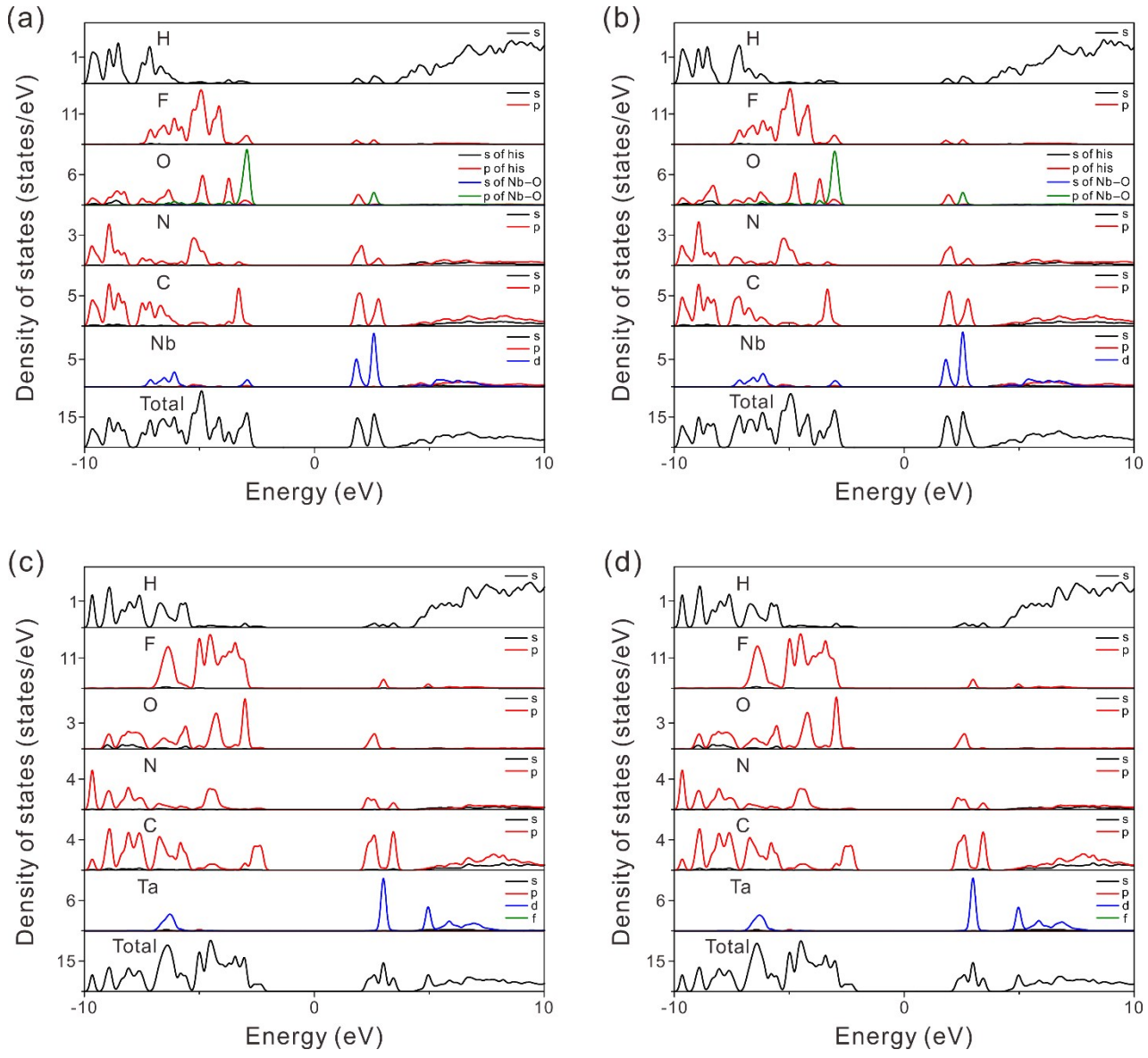

Birefringence calculations. We used a norm-conserving pseudopotential method to calculate the birefringence. The calculations were performed through YAMBO.[9-12] By doing so, the calculated birefringence values of ***Nb*** and ***Ta*** compounds are approximately 0.0365 and 0.049, respectively.

References

1. SAINT 4.05; Siemens Energy and Automation Inc. Madison, WI **1996**.
2. SADABS; Siemens Industrial Automation Inc. Madison, WI **1996**.
3. Sheldrick, G., SHELXS-2013/1, program for the solution of crystal structures. Germany, University of Göttingen **2013**.
4. Sheldrick, G., Crystal structure refinement with SHELXL. *Acta Crystallogr. Sect. C* **2015,** *71*, 3-8.
5. Farrugia, L., WinGX and ORTEP for Windows: an update. *J. Appl. Crystallogr.* **2012,** *45*, 849-854.
6. Giannozzi, P.; Baroni, S.; Bonini, N.; Calandra, M.; Car, R.; Cavazzoni, C.; Ceresoli, D.; Chiarotti, G. L.; Cococcioni, M.; Dabo, I., QUANTUM ESPRESSO: a modular and open-source software project for quantum simulations of materials. *J. Phys.: Condense. Mat.* **2009,** *21*, 395502.
7. Vanderbilt, D., Soft self-consistent pseudopotentials in a generalized eigenvalue formalism. *Phys. Rev. B* **1990,** *41*, 7892.
8. Perdew, J. P.; Burke, K.; Ernzerhof, M., Generalized gradient approximation made simple. *Phy. Rev. Lett.* **1996,** *77*, 3865.
9. G. Adragna, R. Del Sole and A. Marini, *Physical Review B*, 2003, **68**, 165108.
10. A. Marini, R. Del Sole and A. Rubio, *Phys. Rev. Lett.*, 2003, **91**, 256402.
11. M. Rohlfing and S. G. Louie, *Phys. Rev. Lett.*, 1998, **81**, 2312.
12. F. Sottile, V. Olevano and L. Reining, *Phys. Rev. Lett.*, 2003, **91**, 056402.